

# Quasi-stationary North Equatorial Undercurrent jets across the tropical North Pacific Ocean

Bo Qiu,<sup>1</sup> Daniel L. Rudnick,<sup>2</sup> Shuiming Chen,<sup>1</sup> and Yuji Kashino<sup>3</sup>

Received 21 February 2013; revised 16 March 2013; accepted 20 March 2013; published 30 May 2013.

[1] Subthermocline circulation in the tropical North Pacific Ocean (2°N–30°N) is investigated using profiling float temperature-salinity data from the International Argo and the Origins of the Kuroshio and Mindanao Current (OKMC) projects. Three well-defined eastward jets are detected beneath the wind-driven, westward flowing North Equatorial Current. Dubbed the North Equatorial Undercurrent (NEUC) jets, these subthermocline jets have a typical core velocity of 2–5 cm s<sup>-1</sup> and are spatially coherent from the western boundary to about 120°W across the North Pacific basin. Centered around 9°N, 13°N, and 18°N in the western basin, the NEUC jet cores tend to migrate northward by ~4° in the eastern basin. Vertically, the cores of the southern, central, and northern NEUC jets reside on the 26.9, 27.2, and 27.3  $\sigma_\theta$  surfaces, respectively, and they tend to shoal to lighter density surfaces, by about 0.2  $\sigma_\theta$ , as the jets progress eastward. **Citation:** Qiu, B., D. L. Rudnick, S. Chen, and Y. Kashino (2013), Quasi-stationary North Equatorial Undercurrent jets across the tropical North Pacific Ocean, *Geophys. Res. Lett.*, 40, 2183–2187, doi:10.1002/grl.50394.

## 1. Introduction

[2] With the advancement of satellite altimetry in conjunction with in situ observations, our knowledge of the upper ocean circulation has increased significantly over the past two decades. In comparison, information about the subthermocline circulation features remains fragmentary. For the subthermocline Pacific basin, much of the research focus of the past decades has been directed to the equatorial band within the  $\pm 10^\circ$  latitudes. In addition to the alternating equatorial deep jets centered on the equator with a vertical wavelength of several hundred meters [e.g., Firing, 1997; Johnson *et al.*, 2002], alternating zonal jets have also been observed laterally below the permanent thermocline. These laterally aligned jets include the westward Lower Equatorial Intermediate Current on the equator, the eastward Northern and Southern Intermediate Countercurrents at  $\pm 2^\circ$  latitudes, the westward North and South Equatorial Intermediate Current at  $\pm 3^\circ$  latitudes, and the eastward northern and southern secondary Subsurface Countercurrents at  $\pm 5^\circ$  latitudes [e.g., Firing *et al.*, 1998; Rowe *et al.*, 2000; Gouriou *et al.*, 2006].

<sup>1</sup>Department of Oceanography, University of Hawaii at Manoa, Honolulu, Hawaii, USA.

<sup>2</sup>Scripps Institution of Oceanography, La Jolla, California, USA.

<sup>3</sup>Japan Agency for Marine-Earth Science and Technology, Yokosuka, Japan.

Corresponding author: B. Qiu, Department of Oceanography, University of Hawaii at Manoa, Honolulu, HI 96822, USA. (bo@soest.hawaii.edu)

©2013. American Geophysical Union. All Rights Reserved.  
0094-8276/13/10.1002/grl.50394

[3] While all of the above studies focusing on the subthermocline equatorial zonal flows were based on shipboard Acoustic Doppler Current Profiler (ADCP) measurements, the establishment of the International Argo Program in the early 2000s [Roemmich *et al.*, 2009] provides us now with a novel in situ data set to explore the mid-depth circulation signals. Utilizing the drifting information of consecutive float profiles, Cravatte *et al.* [2012] have constructed maps of the mean zonal flows in the 12°S–12°N band of the equatorial Pacific at the float parking depths of 1000 m and 1500 m. They found alternating westward and eastward jets with a meridional scale of ~1.5° and speeds of ~5 cm s<sup>-1</sup>. The jets are generally stronger in the western and central basins and tend to weaken, or disappear, in the eastern basin.

[4] In comparison to the equatorial flow system, basin-scale subthermocline circulation features in the tropical North Pacific Ocean of 10°N–30°N are yet to be explored observationally. As part of the ongoing Origins of the Kuroshio and Mindanao Current (OKMC) project, 10 SOLO-II profiling floats were deployed in the Philippine Sea in August 2011. With a repeat cycle of 5 days, a significant amount of high vertical resolution temperature-salinity (T-S) profiles in the 2000 m upper ocean has been collected in the northwestern Pacific Ocean. By combining the available float T-S data from both the OKMC and Argo projects, we seek in this study to quantify the mid-depth mean flow structures across the entire tropical North Pacific basin.

## 2. Profiling Float Data

[5] All profiling float data available from <http://www.usgodae.org>, including those of the OKMC floats, from January 2001 to October 2012 are analyzed in this study. Within the 0°N–30°N of the North Pacific Ocean of our interest, 1554 floats passed through. Distributions of the floats as a function of space and time are shown in Figure 1. North of 5°N, the data coverage is overall reasonable with the profile density >50 in the 3° × 1° boxes. Temporally, the float data are not biased seasonally and become relatively uniform after 2007. For data quality control, we compare the float-measured T-S data against the 1° × 1° *World Ocean Atlas 2001* climatological data [Conkright *et al.*, 2002]. The T-S data are excluded if they fall outside of the 2 standard deviation envelopes of the local, climatological T-S curve. For the 133,589 profiles that passed the quality control procedure, the T-S data are first interpolated onto a regular 10 m vertical grid between the surface and 2000 m. At each depth, T-S values are then mapped onto a 0.5° latitude and 1° longitude grid using an objective mapping technique. The Gaussian weight function for mapping has a form of  $\exp[-\Delta x^2/2L_x^2 - \Delta y^2/2L_y^2]$ , where  $\Delta x$  and  $\Delta y$  are the zonal and meridional distances between a

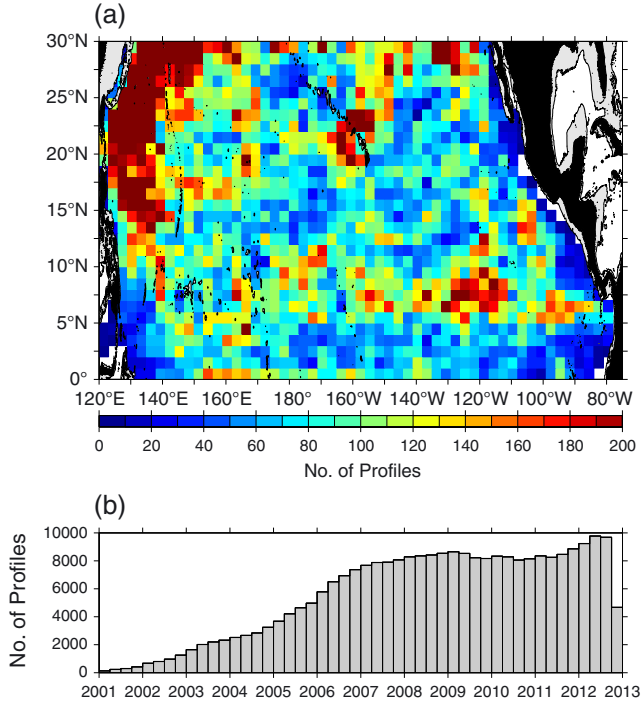


**Figure 1.** (a) Number of T/S profiles in  $3^\circ$  longitude  $\times$   $1^\circ$  latitude boxes of the North Pacific Ocean for the period of January 2001 to October 2012. (b) Histogram of the T/S profiles as a function of years/seasons.

data point and the grid point. For the spatial decorrelation scales,  $L_x = 2^\circ$  in longitude and  $L_y = 0.5^\circ$  in latitude are chosen based on autocorrelations of the mapped subthermocline flow field.

[6] Unlike the previous studies that use the float trajectory data to derive the subthermocline circulation signals [e.g., Cravatte *et al.*, 2012; Qiu *et al.*, 2008; Ollitrault *et al.*, 2006], we choose to describe the geostrophic circulation patterns relative to the 2000 m depth. Our reasons for choosing this method over the float trajectory approach are twofold. First, the wind-driven North Pacific subtropical gyre in the  $10^\circ$ – $30^\circ$ N band is relatively shallow ( $\sim 600$  m) and the flow amplitude at the 2000 m level is on the order of  $0.5 \text{ cm s}^{-1}$ , based on the previously estimated parking depth velocities of Lebedev *et al.* [2007] and Cravatte *et al.* [2012] plus the float-derived geostrophic shears. This magnitude of flow is on par with the uncertainties in estimating the parking depth velocity due to imprecise float position fixes and spatial drifts when a float ascends and descends [e.g., Park *et al.*, 2005; Chen *et al.*, 2007]. The second reason is that the subthermocline jets of our interest are confined to the depth range of 300–1000 m; their structures are largely insensitive to the addition of the 2000 m reference velocity. Given the uncertainties in deriving this latter velocity, we find it more straightforward to construct the three-dimensional circulation pattern in the upper 2000 m with a zero referencing velocity.

### 3. The NEUC Jets

[7] Figure 2 shows the latitude-depth sections of the mean zonal geostrophic velocities along  $130^\circ\text{E}$ – $135^\circ\text{E}$ ,

$175^\circ\text{E}$ – $180^\circ\text{E}$ , and  $150^\circ\text{W}$ – $145^\circ\text{W}$ , respectively. These three sections represent the flow structures typical in the western, central, and eastern North Pacific Ocean. In the wind-driven North Pacific tropical and subtropical gyres, the base of the permanent thermocline is shallow, typically  $\leq 500$  m, and has a density of  $\sim 26.5 \sigma_\theta$ . Along  $130^\circ\text{E}$ – $135^\circ\text{E}$  in the western basin (Figure 2a), upper ocean flows above the permanent thermocline consist of the eastward flowing North Equatorial Countercurrent (NECC) in  $2.5^\circ\text{N}$ – $7.5^\circ\text{N}$  and the broad-scale, westward flowing North Equatorial Current (NEC) in  $7.5^\circ\text{N}$ – $25^\circ\text{N}$ . In between  $17^\circ\text{N}$  and  $25^\circ\text{N}$ , one can detect multiple, surface-trapped Subtropical Countercurrent (STCC) branches that flow eastward and override the NEC [e.g., Kobashi *et al.*, 2006]. The eastward flow north of  $27.5^\circ\text{N}$  in Figure 2a signifies a portion of the northeastward flowing Kuroshio south of Japan. Similar upper ocean flow patterns to Figure 2a can be seen in the central and eastern basins; the exceptions are that the Kuroshio is located north of  $30^\circ\text{N}$  (hence absent in Figures 2b and 2c) and that the surface-trapped STCC along  $150^\circ\text{W}$ – $145^\circ\text{W}$  in the eastern basin appears in the higher latitude of  $25^\circ\text{N}$ – $28^\circ\text{N}$ .

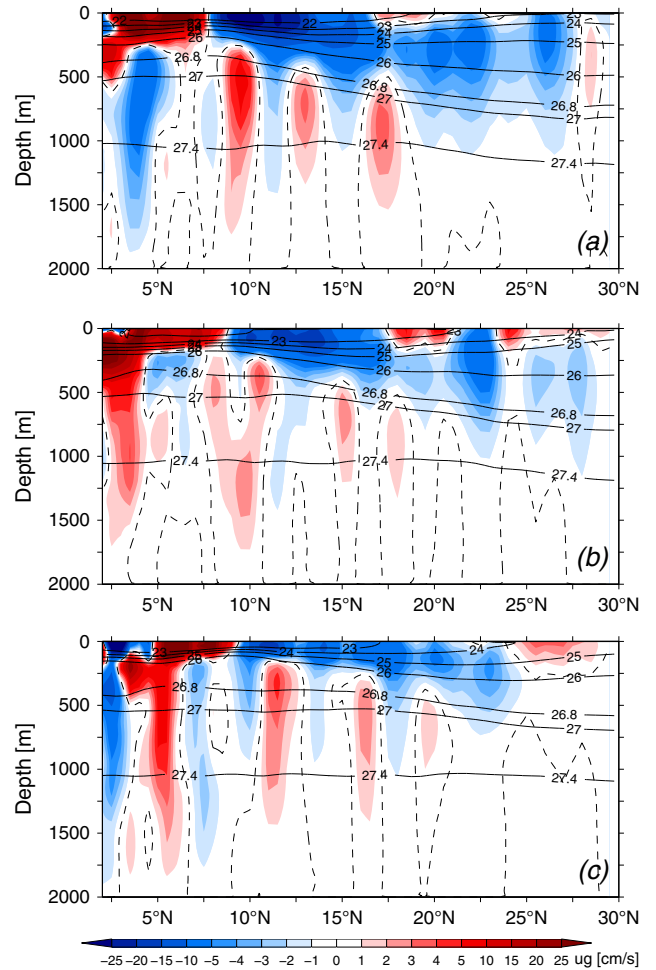


**Figure 2.** Latitude-depth section of density (solid contours, in  $\sigma_\theta$ ) and zonal geostrophic velocity (color shading) along (a)  $130^\circ\text{E}$ – $135^\circ\text{E}$ , (b)  $175^\circ\text{E}$ – $180^\circ\text{E}$ , and (c)  $150^\circ\text{W}$ – $145^\circ\text{W}$ . The geostrophic velocity is referenced to 2000 m and dashed lines denote the zero velocity contours.

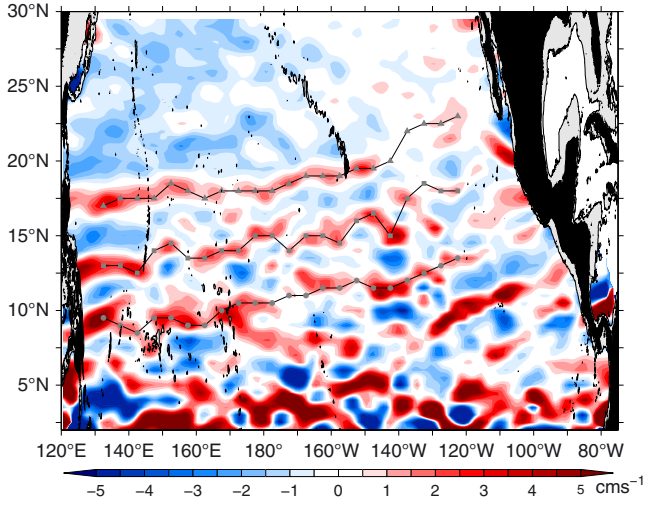


**Figure 3.** Distribution of zonal geostrophic velocity averaged between the 26.8–27.4  $\sigma_\theta$  density surfaces. Grey symbols denote the locations of the NEUC jet cores that are derived based on the zonal geostrophic flow patterns averaged in each 5° longitude segment (see Figure 2 for the three representative segments).

[8] Beneath the permanent thermocline of the westward flowing NEC, Figure 2a shows that there exist three, well-defined, eastward-flowing jets with cores centered around 9°N, 13°N, and 18°N, respectively. The cores of these subthermocline jets reside on the 26.9–27.3  $\sigma_\theta$  density surfaces and their velocities are on the order of 4–5  $\text{cm s}^{-1}$ . Though inconspicuous in Figure 2a, there exists a tendency for the jet cores to progressively shift from a lighter to denser density surface from south to north. The three subthermocline jets can be similarly identified beneath the westward flowing NEC along the 175°E–180°E and 150°W–145°W sections (Figures 2b and 2c). Compared to Figure 2a, the cores of the three jets tend to shift northward and onto a lighter density surface, and their speed tends to drop down to 1–2  $\text{cm s}^{-1}$ , when moving toward the east.

[9] Beneath the eastward flowing NECC, Figures 2b and 2c reveal the presence of two additional, eastward flowing subthermocline jets at 2°N–3°N and ~5°N. These two jets correspond to the eastward off-equatorial jets along 2°N and 5°N identified by Cravatte *et al.* [2012] based on the analyses of Argo float trajectories at 1000 m. Following the nomenclature adopted by Gouriou *et al.* [2006] for the Southern Hemisphere current system, we can refer to the subthermocline equatorial jets at 2°N and 5°N as the Northern Intermediate Countercurrent (NICC) and the northern secondary Subsurface Countercurrent, respectively. Although the subthermocline jet at ~9°N was detected by Cravatte *et al.* [2012], the two northern jets at 13°N and 18°N shown in Figure 2 have not been captured before. Given their presence beneath the westward flowing NEC and their common dynamic properties (to be discussed below), we propose in this study to name these three subthermocline jets collectively as the North Equatorial Undercurrent (NEUC) jets.

[10] To explore the longitudinal continuity of the NEUC jets, we plot in Figure 3 the distribution of zonal geostrophic velocity averaged between the 26.8–27.4  $\sigma_\theta$  density surfaces. To aid the jet identification, we have superimposed

on Figure 3 by grey marks the locations of the NEUC jet cores that are derived from the  $U_g(y, z)$  profiles in each 5° longitude segment, similar to those presented in Figure 2. A roughly zonally persistent  $U_g > 0$  band can be seen along 17°N–20°N from the western boundary to east of the Hawaiian Islands. This band corresponds to the northern NEUC jet depicted in Figure 2. The central NEUC jet is discernible in Figure 3 as the positive  $U_g$  band slanting southwest-northeastward along 13°N–17°N. For the southern NEUC jet, it runs roughly along 9°N–10°N west of the dateline and veers northeastward further to the east. From Figure 3, it is possible to identify a fourth SW-NE tilting zonal jet in the eastern North Pacific basin along ~10°N. When compared with the three NEUC jets described above, its extension into the western basin appears less persistent.

[11] Due to the uneven data availability in space (recall Figure 1a), the NEUC jets in Figure 3 can appear zonally disconnected in various locations. This may raise concern about the robustness of the poleward shift of the three NEUC jets. To address this concern, we plot in Figure 4a the salinity distribution on the 27.0  $\sigma_\theta$  surface from the float measurements. Although distorted laterally, the paths of the three NEUC jets follow roughly in parallel with the SW-NE tilting isohaline contours. Given that salinity

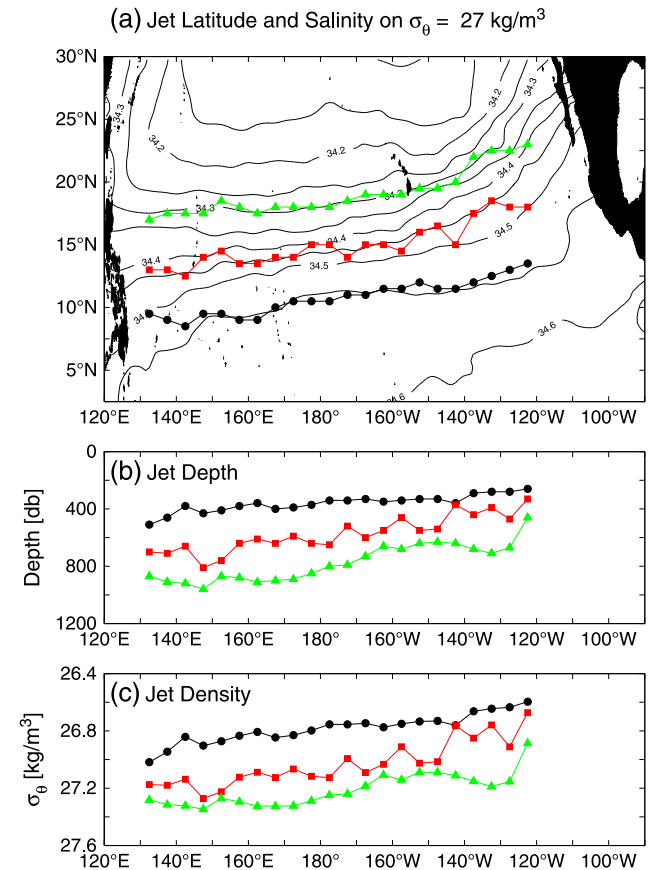


**Figure 4.** (a) Salinity distribution on the 27.0  $\sigma_\theta$  density surface. The superimposed symbols denote the locations of the NEUC jet cores. (b and c) The depth and density of the NEUC jet cores as a function of longitude. In all plots, green, red, and black symbols denote the properties for the northern, central, and southern NEUC jets, respectively.

is largely a passive tracer below the permanent thermocline, this parallel distribution provides independent evidence for the poleward tilt of the NEUC jets from west to east.

[12] In Figures 4b and 4c, we plot the depth and density of the NEUC jet cores as a function of longitude. As the NEUC jets migrate poleward toward east, its core shifts simultaneously to a shallower depth and a lighter density surface. These characteristics of the NEUC jets mirror very well the flow properties of the overlying NEC across the North Pacific basin. Specifically, the wind-driven NEC above the permanent thermocline has a similar NE-SW tilt in the region of 9°N–20°N and, as can be verified in Figure 2, the depth of the NEC becomes shallower and its lower boundary shoals to a lighter density surface from west to east.

#### 4. Discussion

[13] Based on the available profiling float T-S data, our analysis of the three-dimensional circulation in the tropical North Pacific Ocean has detected the presence of three eastward flowing jets immediately beneath the permanent thermocline of the NEC. These three subthermocline jets are zonally coherent from the western boundary to about 120°W and are centered approximately along 9°N, 13°N, and 18°N in the western North Pacific basin. The spatial characteristics of these jets, i.e., veering poleward and shoaling to lighter density surfaces from the western to eastern basin, are similar to those of the overlying NEC. Given these similarities, it is proposed in this study to name these newly detected subthermocline jets the North Equatorial Undercurrent (NEUC) jets.

[14] Eastward flows below the NEC within the western North Pacific basin have been observed sporadically in the past. For example, *Toole et al.* [1988] presented evidence for subthermocline eastward flows at 10°N and 12°N from two hydrographic surveys along 130°E. Based on a hydrographic cruise along the same longitude, *Hu and Cui* [1991] observed subthermocline eastward flows at 12°N and 18°N. A subthermocline eastward jet was identified to be a *time-mean* feature at ~10°N by *Qiu and Joyce* [1992] based on long-term hydrographic surveys along 137°E. Using the multiple hydrographic surveys along 130°E, *Wang et al.* [1998] adopted the name of NEUC to describe the eastward flow beneath the NEC. In addition to these studies using the hydrographic data, existence of the subthermocline eastward flows is also evident in recent shipboard acoustic Doppler current profiler (ADCP) measurements [*Kashino et al.*, 2009; *Dutrieux*, 2009]. Because the ADCP measurements only extend to 600 m, they capture often the top portions of the NEUC jets. In short, while their presence is hinted in the existing literature, it is the global profiling float data that provided us a means to comprehensively examine the three NEUC jets across the entire North Pacific basin.

[15] It is worth emphasizing that the three NEUC jets shown in Figure 3 remain largely unchanged, or quasi-stationary, when the  $U_g$  fields are constructed using the T-S data from 2001–2008 and 2009–2012 separately (figure not shown). Dynamically, it is also interesting to note that the SW-NE veering by the NEUC jets is opposite to the

NW-SE veering by the eastward subthermocline jets identified by *Cravatte et al.* [2012] at 2°N and 5°N in the equatorial Pacific Ocean. This opposite tilting may reflect the different background mean circulation structures the NEUC jets versus the off-equatorial jets are embedded in. It could also imply that the equatorial and tropical subthermocline jets have different forcing mechanisms.

[16] Several studies based on high-resolution ocean general circulation model simulations have indicated the possibility that alternating zonal jets in the tropical and midlatitude Pacific Ocean are generated spontaneously by geostrophic turbulence on a  $\beta$ -plane [e.g., *Nakano and Hasumi*, 2005; *Maximenko et al.*, 2005; *Richards et al.*, 2006]. It is worth emphasizing the NEC along 9°N–18°N across the North Pacific basin is a band with relatively low mesoscale eddy activity [see, e.g., *Ducet et al.*, 2000, Plate 8]. Dynamically, this is due to the resistance of the NEC system against baroclinic instability [*Qiu*, 1999]. With this low level of mesoscale eddy variability, it will be important for future studies to quantify whether the nonlinear rectification by  $\beta$ -plane geostrophic turbulence [*Rhines*, 1975] is a viable mechanism for generating the NEUC jets.

[17] Using a coupled atmosphere-ocean general circulation model, *Taguchi et al.* [2012] have recently found subthermocline zonal jets existing in the tropical central South Pacific Ocean. In accordance with the analysis by *Kessler and Gourdeau* [2006], *Taguchi et al.* [2012] demonstrated that these zonal jets are in approximate sverdrup balance with the collocated, small-scale surface wind stress curl forcing (the sverdrup prediction explains about half the amplitude of the jets). By examining the impact of sea surface temperature anomalies upon the overlying atmosphere, they further showed that the small-scale wind stress curl signals could be enhanced through feedback by the sverdrup zonal jets. Following these South Pacific Ocean studies, we have calculated the sverdrup zonal flows in the North Pacific basin based on the satellite-derived QuikSCAT wind data. No small-scale wind stress curl forcing was found to be collocated with the NEUC jets. Though lacking small-scale features, the wind stress curl forcing has large amplitudes, especially in the annual frequency band, along the 9°N–20°N band in the North Pacific basin. It will be important for future studies to quantify how this time-varying surface wind forcing can result in rectified subthermocline circulations.

[18] **Acknowledgments.** We thank the anonymous reviewers whose detailed comments helped improve an early version of the manuscript. The Argo profiling float data used in this study were provided by the US-GODAE Argo Global Data Assembly Center. This study was supported by the ONR project Origins of the Kuroshio and Mindanao Current (OKMC): N00014-10-1-0267 (BQ and SC) and N00014-10-1-0273 (DLR).

[19] The Editor thanks two anonymous reviewers for their assistance in evaluating this paper.

#### References

- Chen, S., B. Qiu, and P. Hacker (2007), Profiling float measurements of the recirculation gyre south of the Kuroshio Extension in May to November 2004, *J. Geophys. Res.*, *112*, C05023, doi:10.1029/2006JC004005.
- Conkright, M. E., R. A. Locarnini, H. E. Garcia, T. D. O'Brien, T. P. Boyer, C. Stephens, and J. I. Antonov (2002), *World Ocean Atlas 2001: Objective Analyses, Data Statistics, and Figures, CD-ROM Documentation*, 17 pp., National Oceanographic Data Center, Silver Spring, MD.

- Cravatte, S., W. S. Kessler, and F. Marin (2012), Intermediate zonal jets in the tropical Pacific Ocean observed by Argo floats, *J. Phys. Oceanogr.*, *42*, 1475–1485.
- Ducet, N., P.-Y. Le Traon, and G. Reverdin (2000), Global high-resolution mapping of ocean circulation from TOPEX/Poseidon and ERS-1 and -2, *J. Geophys. Res.*, *105*, 19,477–19,498.
- Dutrieux, P. (2009), Tropical western Pacific currents and the origin of intraseasonal variability below the thermocline, PhD thesis, University of Hawaii, pp. 122.
- Firing, E. (1997), Deep zonal currents in the central equatorial Pacific, *J. Mar. Res.*, *43*, 791–812.
- Firing, E., S. E. Wijffels, and P. Hacker (1998), Equatorial subthermocline currents across the Pacific, *J. Geophys. Res.*, *103*, 21,413–21,424.
- Gouriou, Y., T. Delcroix, and G. Eldin (2006), Upper and intermediate circulation in the western equatorial Pacific Ocean in October 1999 and April 2000, *Geophys. Res. Lett.*, *33*, L10603, doi:10.1029/2006GL025941.
- Hu, D., and M. Cui (1991), The western boundary current of the Pacific and its role in the climate, *Chin. J. Oceanol. Limnol.*, *9*, 1–14.
- Johnson, G. C., E. Kunze, K. E. McTaggart, and D. W. Moore (2002), Temporal and spatial structure of the equatorial deep jets in the Pacific Ocean, *J. Phys. Oceanogr.*, *32*, 3396–3407.
- Kashino, Y., N. Espana, F. Syamsudin, K. J. Richards, T. Jensen, P. Dutrieux, and A. Ishida (2009), Observations of the north equatorial current, Mindanao current, and the Kuroshio current system during the 2006/07 El Niño and 2007/08 La Niña, *J. Oceanogr.*, *65*, 325–333.
- Kessler, W. S., and L. Gourdeau (2006), Wind-driven zonal jets in the South Pacific Ocean, *Geophys. Res. Lett.*, *33*, L03608, doi:10.1029/2005GL025084.
- Kobashi, F., H. Mitsudera, and S.-P. Xie (2006), Three subtropical fronts in the North Pacific: Observational evidence for mode water-induced subsurface frontogenesis, *J. Geophys. Res.*, *111*, C09033, doi:10.1029/2006JC003479
- Lebedev, K. V., H. Yoshinari, N. A. Maximenko, and P. W. Hacker (2007), YoMaHa'07: Velocity data assessed from trajectories of Argo floats at parking level and at the sea surface, *IPRC Technical Note*, *4*, 16 pp.
- Maximenko, N. A., B. Bang, and H. Sasaki (2005), Observational evidence of alternating zonal jets in the world ocean, *Geophys. Res. Lett.*, *32*, L12607, doi:10.1029/2005GL022728.
- Nakano, H., and H. Hasumi (2005), A series of zonal jets embedded in the broad zonal flows in the Pacific obtained in eddy-permitting ocean general circulation models, *J. Phys. Oceanogr.*, *35*, 474–488.
- Ollitrault, M., M. Lankhorst, D. Fratantoni, P. Richardson, and W. Zenk (2006), Zonal intermediate currents in the equatorial Atlantic Ocean, *Geophys. Res. Lett.*, *33*, L05605, doi:10.1029/2005GL025368.
- Park, J. J., K. Kim, B. A. King, and S. C. Riser (2005), An advanced method to estimate deep currents from profiling floats, *J. Atmos. Oceanic Technol.*, *22*, 1294–1304.
- Qiu, B. (1999), Seasonal eddy field modulation of the North Pacific Subtropical Countercurrent: TOPEX/POSEIDON observations and theory, *J. Phys. Oceanogr.*, *29*, 2471–2486.
- Qiu, B., and T. M. Joyce (1992), Interannual variability in the mid- and low-latitude western North Pacific, *J. Phys. Oceanogr.*, *22*, 1062–1079.
- Qiu, B., S. Chen, P. Hacker, N. Hogg, S. Jayne, and H. Sasaki (2008), The Kuroshio Extension northern recirculation gyre: Profiling float measurements and forcing mechanism, *J. Phys. Oceanogr.*, *38*, 1764–1777.
- Rhines, P. B. (1975), Waves and turbulence on a beta-plane, *J. Fluid Mech.*, *69*, 417–443.
- Richards, K. J., N. A. Maximenko, F. O. Bryan, and H. Sasaki (2006), Zonal jets in the Pacific Ocean, *Geophys. Res. Lett.*, *33*, L03605, doi:10.1029/2005GL024645.
- Roemmich, D., et al. (2009), The Argo program: Observing the global ocean with profiling floats, *Oceanography*, *22*, 34–43.
- Rowe, G. D., E. Firing, and G. C. Johnson (2000), Pacific equatorial subsurface countercurrent velocity, transport, and potential vorticity, *J. Phys. Oceanogr.*, *30*, 1172–1187.
- Taguchi, B., R. Furue, N. Komori, A. Kuwano-Yoshida, M. Nonaka, H. Sasaki, and W. Ohfuchi (2012), Deep oceanic zonal jets constrained by fine-scale wind stress curls in the South Pacific Ocean: A high-resolution coupled GCM study, *Geophys. Res. Lett.*, *39*, L08602, doi:10.1029/2012GL051248.
- Toole, J. M., E. Zou, and R. C. Millard (1988), On the circulation of the upper waters in the western equatorial Pacific Ocean, *Deep Sea Res., Part A*, *35*, 1451–1482.
- Wang, F., D. Hu, and H. Bai (1998), Western boundary undercurrents east of the Philippines, *Proceedings of the 4th Pacific Ocean Remote Sensing Conference (PORSEC)*, Qingdao, China, 551–556.